Functional specialization under multidimensional tradeoffs

André Amado[‡] and Paulo R. A. Campos[‡]

December 10, 2018

[‡]Departamento de Física, Universidade Federal de Pernambuco, 50740-560 Recife-PE, Brazil

Corresponding author: Paulo R. A. Campos

Running Title: multidimensional tradeoffs

e-mail: paulo.acampos@ufpe.br

Keywords: evolutionary theory, tradeoff, trait, adaptation

Abstract

Although tradeoffs are expected to play an essential role in shaping the diversity in a community, their effects remain relatively nebulous and notoriously difficult to assess. This is especially true under the occurrence of multiple tradeoffs. To address this issue, we develop a resource-based model that encompasses multiple tradeoffs mediated by the acquisition and processing of the resources. The model considers a spatially structured population of microbial organisms that can grow on an arbitrary number of resources, which come into the system at a constant rate and diffuse through the environment. The individuals can adopt a variety of strategies constrained by the tradeoffs and during replication the daughter cells can present slightly different behavior compared to the parental cells, which renders the model adaptive. We assess population sizes and levels of functional specialization. This allows us to infer the effect of different tradeoff scenarios as well as the impact of resource and space availability.

1 Introduction

Most natural environments harbor a great diversity of microbial life (Hibbing et al. 2010; Gibbons and Gilbert 2015). In those environments, microbes are typically surrounded by different strains and species with whom they compete for nutrients and space. Inside the colonies, the microbes usually express many different phenotypes in such a way that they can thrive in outcompeting and displacing their neighbors (Ghoul and Mitri 2016). The outcome of this competition and the fate of the distinct evolutionary strategies, under the constraints of tradeoffs, are greatly driven by the ecological scenarios (Ghoul and Mitri 2016; de Oliveira et al. 2018; Hoyle et al. 2008). Many works explore how the shape of the tradeoffs together with the ecological scenario can affect the evolutionary predictions (de Oliveira et al. 2018; Hoyle et al. 2008). Other works further suggest that even the shape of the tradeoff relationship responds to environment changes (Jessup and Bohannan 2008).

A fundamental aspect of species that must be acknowledged in the study of the emergence of functional specialization is that species are not uniform entities, but rather adapt to local environmental conditions, thus rendering patterns of population differentiation owing to their phenotypic plasticity (Valladares et al. 2014), which is understood as the ability of one genotype to produce more than one phenotype when exposed to different environments (Ghalambor et al. 2007). In fact, the ability of organisms to settle their phenotype to changing conditions is well established as a central mechanism, in both microevolutionary and macroevolutionary scales (Kümmerli et al. 2009; Chevin et al. 2013; Beier et al. 2015; Kelly et al. 2012; Matesanz et al. 2010; Nicotra et al. 2010). Populations facing different environmental conditions are dissimilar in their phenotypic responses (Sultan and Spencer 2002).

Tradeoffs are considered to have a central role in determining the patterns of species diversity in ecological communities (Kneitel and Chase 2004), including the diversity in the microbial world (Ferenci 2016). Tradeoffs constrain the range of phenotypic options that are open to organisms, and result from a number of physical and biological mechanisms (Garland 2014). On the one hand, tradeoffs curb the adaptive potential of organisms, but on the other, act as a driving mechanism for diversification in the context of environmental variation (Østman et al. 2014).

Despite their importance to life-history theory, quantifying tradeoffs requires longterm observation and modeling and are subject to

several limitations (Pease and Bull 1988). This problem is even more subtle when multidimensional tradeoffs exist (Edwards, Klausmeier, and Litchman 2011; Lancaster, Hazard, Clobert, and Sinervo 2008). The existence and interplay of multiple tradeoffs and their consequences to the degree of functional specialization are addressed in this contribution. The tradeoffs are here modelled as surfaces and curves in trait space, thus representing the constraints between the variables. Our approach is developed within a resource-based modelling framework, and thereby we are concerned with the metabolic properties of the individuals. In particular, two well-acknowledged tradeoffs in the literature are considered: between resource uptake rates and the rate-yield tradeoff (Litchman et al. 2015). The latter one defines a constraint between the rate at which a given resource is uptaken and the efficiency of the process of conversion of those seized resources into ATP (energy). The curvatures of the surfaces and curves in trait space can be tuned, thus allowing us to cover a broad spectrum of possible shapes and curvatures. As aforesaid, this matter is of great relevance especially in the face of our knowledge from classical ecological models that deal with two-traits relationships (Egas et al. 2004; Hoyle et al. 2008). These classical ecological models state that specialization is expected under convex curves, whereas the generalist strategy is favored under concave relationships. So, many questions arise upon the occurrence of multivariate tradeoff patterns, especially those involving different classes of tradeoffs (distinct biological quantities). For instance, what is the evolutionary outcome whether there exist tradeoffs of opposing curvatures? And what about multidimensional tradeoffs involving different quantities? Do we have any kind of hierarchy regarding the tradeoffs? Those types of questions we address in the current contribution.

In the Sec. 2, we describe the model used to address the aforedescribed problem and the technical aspects that underlie it. This is followed by a description of the results in section 3. Finally, we present our concluding remarks.

2 Materials and Methods

The present work is developed within the framework of a resource-based modelling. It assumes the existence of biophysical limitations that impose constraints between resource uptake rates and between resource uptake rate and the corresponding performance of the process of conversion of resource into energy. These two types of tradeoffs are well established and documented in the literature (Pfeiffer et al. 2001;

Litchman et al. 2015). The present contribution aims to comprehend how the entanglement of multiple tradeoff relationships affects the patterns of the functional specialization. With this in mind, one assumes that different types of resources are available to the individuals. The number of resource types is equal to N_r, and the inflow of those resources are denoted by $R^1, R^2, \ldots, R^{N_r}$. The population is assumed to be spatially structured, and thereby the individuals are arranged over a two-dimensional lattice of linear size L. At most a single individual can lie in each site of the lattice, and so each site can be either occupied or unoccupied. The N_r resources diffuse over the lattice, following a discretized version of the diffusion equation, i.e.,

$$\frac{dS^k(r,t)}{dt} = D\,\nabla^2 S^k(r,t), \tag{1}$$

where D is a diffusion constant, and $S^k(r,t)$ denotes the amount of resource R^k at position r at time t. One must be careful about the conditions for stability of the discretized version, which requires that $\Delta t \leq \frac{(\Delta x)^2}{D}$. The flow of a given resource will be largest in the direction of the largest gradient.

The individuals are characterized by their uptake rates A^k, with $k = 1, \ldots, N_r$, and their respective returns η^k, which is the yield of the process that converts biochemical energy from nutrients into energy, here taken as a direct measure of growth rate. In a microevolutionary scale, the biochemical energy stems from some type of sugar, for instance, glucose, which in its turn will be converted into adenosine triphosphate (ATP), which will be used to carry out all the biochemical processes inside the cell.

Individuals can only grab resources in their location. At each time step Δt, individuals lying on position i, j of the lattice will seize an amount of the resource R^k equal to

$$J^k_{i,j} = A^k_{i,j} \frac{S^k_{i,j}}{S^k_{i,j} + A^k_{i,j}\Delta t}. \tag{2}$$

The amount of resource is calculated for each resource type. The above equation is based on Monod and Michaelis-Mentes formulations (Rockwood 2015). Once the resources are captured by the individual, they will subsequently be converted into energy. Note that all resources types are not equally processed by the individual, as each one involves a different metabolic machinery, with their own constraints. So, it sounds natural to associate with each resource R^k a return η^k, which will tell us the amount of energy extracted from that resource amount. Borrowing ideas from the microbial world, the amount of

energy due to resource R^k will be

$$\Delta E_{i,j}^k = \sum_k J_{i,j}^k \Delta t \left[\eta_{i,j}^k E_{max} + (1 - \eta_{i,j}^k) E_{min}) \right] \tag{3}$$

with the total change of internal energy taken as

$$\Delta E_{i,j} = \sum_{k=1}^{N_r} \Delta E_{i,j}^k. \tag{4}$$

The sum is taken over all resource types. As reference values we adopt $E_{\max} = 36$ and $E_{\min} = 2$. $E_{\max}$ is attained when one has maximum efficiency, $\eta^k = 1$, whereas $E_{\min}$ corresponds to a lower bound, when $\eta^k = 0$. Those values are inspired in the metabolic machinery of single-celled organisms, such as bacteria and yeast, where the inneficient mode of metabolism (fermentation) yields typically 2 ATP molecules per glucose molecule, whereas the efficient mode of metabolism, dubbed cellular respiration, yields up to 36 ATP molecules from a single glucose molecule (Campbell and Farrell 2006).

Owing to biological and physical constraints, individuals cannot optimize all the quantities, A^k and η^k with $k = 1, \ldots, N_r$, simultaneously. As will be explained later, these quantities are subject to tradeoffs. Our approach is adaptive, i.e., the individuals' phenotypic traits are subject to changes, providing different responses in their interaction with the environment. Those individuals that are capable of producing energy at a faster pace can thrive and their evolutionary strategies can thus spread, at least locally, as the environment is not expected to be uniform.

2.1 Biological life cycle

Every time step, there is a total inflow of resource ΔS into the system (lattice), which is primarily partitioned into n_{loc} distinct locations over the lattice. For each resource type, the amount of resource per time step is $\Delta S/N_r$, and the set of locations for each type is chosen independently. In the next stage, the resources diffuse over the lattice in a process that follows the discretized version of the diffusion equation, Eq. (1).

The following phase concerns the biological cycle, in which the individuals first seize a fraction of the resources which are available in their local site (Eq. (2)), which in turn will result in an increase in its energy reservoir (biomass). Reproduction (cell division, in a microevolutionary view) will take place every time the individual's energy level reaches the threshold value E_{split}. During cell division, the parental

cell divides into two cells with half of its energy level each. One of the cells remains in the focal position, whereas the second daughter cell will occupy an unoccupied site in the neighborhood of the focal cell. If there is no empty site in its neighborhood, the daughter cell will randomly replace one of its neighbors. The daughter cells are not metabolically identical to the parental cell, but presents slightly different values from the parental cell due to the phenotypic plasticity of the organisms. This mechanism will be described in more detail in the next section. In this sense, our model is adaptive, as the individuals with better phenotypic responses to the local environment are more likely to thrive, as they can better exploit the available resources and use their metabolic machinery to directly increase the reproductive rate, hence locally spreading.

The final stage regards the process of cell death, in which individuals die at a constant rate ν.

2.2 The tradeoff relationships

In the current work, we are concerned with tradeoff relationships affecting metabolic properties of the individuals. Within the perspective of resource handling, two types of tradeoffs are acknowledged, those establishing constraints between resource uptake rates, $A_j \times A_k$, and for each resource type a tradeoff between the resource uptake rate and its corresponding return, $A_j \times \eta_j$. This set of pairwise relations altogether results in a multidimensional coupling as the change in one of those variables leads to changes of all other quantities. A simpler and more elegant formulation is to define a surface in trait space, thus representing the allowed region of phenotypic values stemming from physical and biological constraints. Through the process of phenotypic variation during reproduction, different phenotypic responses are verified, and those that are locally and instantaneously more advantageous can become established.

We will follow this latter formulation, which will be detailed below. An individual can be represented by a vector in trait space, $\vec{P} = (\vec{A}, \vec{\eta})$, with $\vec{A} = (A_1, A_2, \ldots, A_{N_r})$ and $\vec{\eta} = (\eta_1, \eta_2, \ldots, \eta_{N_r})$, hence giving rise to a $2N_r$-dimensional space. We will assume no explicit relationship between the efficiencies $\eta_1, \eta_2, \ldots, \eta_{N_r}$, but rather they are a consequence of their corresponding uptake rates. On the other hand, in the N_r-dimensional subspace $\vec{A}$, the tradeoff relationships among the resource uptake rates, A_k with $k = 1, 2, \ldots, N_r$, will be described by a surface in the subspace $\vec{A}$.

At this point, we will make use of an adaptation of a family of polynomial functions, known as Bézier functions (Farin et al. 2002;

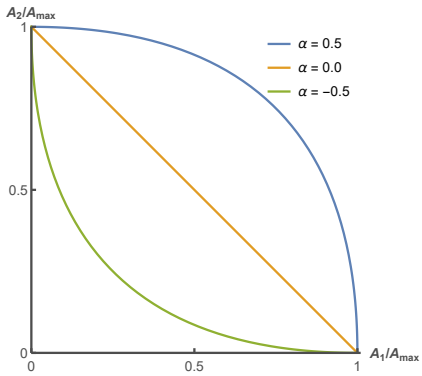

Figure 1: A model of two-resources. Tradeoff between A_1 and A_2 for $\alpha = -0.5$ (green curve), $\alpha = 0$ (orange curve), $\alpha = 0.5$ (blue curve).

Chen and Wang 2003). In n dimensions, a point in the surface is parametrized by

$$\vec{A}\left(\vec{t}\right) = \sum_{i=1}^{n} \left[t_i^2\, \vec{e}_i + (\alpha_{uptake} + 1/2) \sum_{j \neq i} t_i t_j\ (\vec{e}_i + \vec{e}_j) \right] \tag{5}$$

$$= \sum_{i=1}^{n} \left[t_i^2\, \vec{e}_i + 2\,(\alpha_{uptake} + 1/2) \sum_{j > i} t_i t_j\ (\vec{e}_i + \vec{e}_j) \right] , \tag{6}$$

where $\vec{e}_k$ is a unit vector in the k-direction, with k corresponding to a resource index, and the condition $\sum_{i=1}^{n} t_i = 1$ should be respected. The full set of unit vectors $\{\vec{e_k}\}$ defines a complete orthonormal basis in the subspace $\mathcal{A}$. The parameter α_{uptake} determines the shape of the surface. Therefore, to fully parametrize the system $n-1$ variables are necessary. In terms of its components, $(A_1, A_2, \ldots, A_{N_r})$, the above equation can be rewritten as

$$A_k\left(\vec{t}\right) = \vec{e}_k \cdot \vec{A}\left(\vec{t}\right) = \sum_{i=1}^{n} \left[t_i^2\, \delta_{ik} + (\alpha_{uptake} + 1/2) \sum_{j \neq i} t_i t_j\ (\delta_{ik} + \delta_{jk}) \right] \tag{7}$$

$$= (2\alpha_{uptake} + 1)\, t_k - 2\alpha_{uptake}\, t_k^2 , \tag{8}$$

which facilitates its numerical implementation.

In order to determine the efficiency η_k associated with resource of type k, we also assume a dependence similar to those between the uptake rates, $\{A_k\}$, with the efficiency η being determined by the

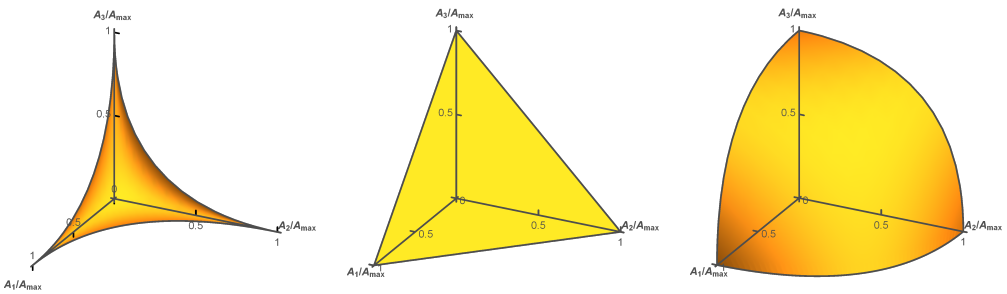

Figure 2: A model of three-resources. Tradeoff between A_1, A_2 and A_3 for $\alpha = -0.5$ (left panel), $\alpha = 0$ (middle panel), $\alpha = 0.5$ (right panel).

equation,

$$\eta_i = \frac{2\alpha_{yield}A_i - 1 + \sqrt{(1+2\alpha_{yield})^2 - 8\alpha_{yield}A_i}}{2\alpha_{yield}}, \tag{9}$$

which basically means that the functional dependence between A and η is similar to the dependence among the set of values $\{A_k\}$, though restricted to two variables. As expected, in the limit $\alpha \to 0$, which corresponds to a linear dependence, the above equation reduces to $\eta_i = 1 - A_i$.

As previously discussed, every time a reproduction event occurs, the daughter cell is metabolically distinct from the parental cell. This step is implemented by randomly picking a single parameter t_i, hence being slightly altered by an amount δt_i, which is a random gaussian distributed variable with mean zero and standard deviation $\sigma = 0.01$. The remaining parameter are then adjusted to obey the condition $\sum_i t_i = 1$. The following step is to recalculate the resource uptake rates from the set of $\{t_k\}$-values, and their corresponding efficiencies η are promptly evaluated from Eq. (9).

The parameter α_{uptake} and α_{yield} play a key function as they rule about the shape of the tradeoff relationships. Negative values of α generates convex surfaces, whereas positive values leads to concave surfaces. When case $\alpha = 0$, the variables are linked by linear relations. Figures. 1 and 2 show intances of the surfaces produced through the Bézier functions. In the plots, the resource uptake rates are rescaled by their maximum value, $A_k/A_{\max}$.

3 Results

In this section we will present the simulation results, aiming to determine the levels of functional specialization under quite distinct sce-

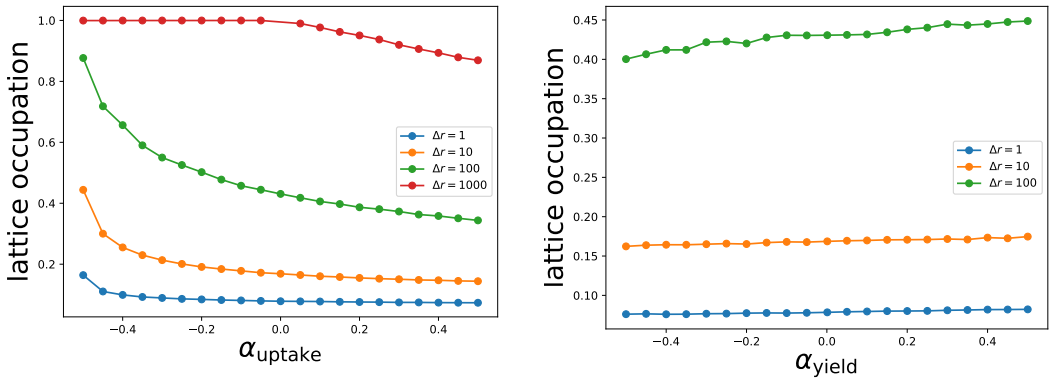

Figure 3: Lattice occupation as a fraction of the maximum lattice capacity for several values of resource input rate ΔR. The left panel depicts the dependence with α_{uptake} for constant $\alpha_{\text{yield}} = 0$ and the right panel shows the dependence with α_{yield} for constant $\alpha_{\text{uptake}} = 0$. The parameters are $N = 3$, $\nu = 0.01$, $A_{\text{max}} = 10$, $L = 100$, $D = 0.2$, $\Delta t = 0.1$ and $\Delta x = 1$. Each point consists of an average over 100000 time units, sampled every 5 time units, taken from 50 independent configurations.

narios. In our simulations, unless stated otherwise, the linear system size is $L = 100$, in such a way that there are $N = L \times L$ sites. The number of source spots for each resource type is $n_{loc} = 100$, and the diffusion constant D is $D = 0.2$. The measurements are taken after the system has reached an equilibrium regime.

First, it is important to determine how the population size is influenced by the variables of the model. In the left panel of Fig. 3, the dependence of the population size, here expressed as the fraction of occupied sites of the lattice, on the curvature parameter α_{uptake} is explored. Meanwhile, α_{yield} is set at $\alpha_{yield} = 0$, meaning a linear relationship between resource uptake rate and the efficiency η for each resource type. Different values of resource input ΔR are simulated. As expected, the population size is an increasing function of ΔR. In fact, the lattice becomes fully or almost fully populated when either ΔR is large or has intermediate values and α_{uptake} takes very negative values. Under these conditions, space limitation is expected to play an important role. In a nutshell, one may also conclude that the occupation fraction drops off with the curvature parameter α_{uptake}, though for small resource input ΔR it remains roughly constant over a broad range of α_{uptake}. If looked at isolatedly, one would say that negative values of α_{uptake} favor the rise of specialized individuals in the resource uptake of one or a few resource types. Under this perspective,

those results seem to demonstrate that upon functional specialization larger populations can be accommodated. On the other hand, we observe that by holding α_{uptake} and varying α_{yield} (right panel of Fig. 3) one deduces that α_{yield} has a less prominent role in regulating the population size.

In order to corroborate the above conjecture, the left panel of Fig. 4 shows the level of specialization in the resource uptake against the curvature parameter α_{uptake}. Once again, one has $N_r = 3$ resources and $\alpha_{yield} = 0$. From the plot, we find out that the level of specialization is a monotonic decreasing function of α_{uptake}, allowing us to associate increased population sizes with higher levels of specialization in the resource uptake. In our metric, the specialization level is defined in the range $(0, M_{uptake})$, where $M_{uptake} = N_r \times (N_r - 1)/2$, which corresponds to the number of pairwise relations of the class $A_j \times A_k$. Hence, we examine if the ratio A_j/A_k either the condition $A_j/A_k > r_{spec}$ or $A_j/A_k < 1/r_{spec}$, which upholds specialization for the considered pair of uptake rates. Therefore, each pairwise relation $A_j \times A_k$ contributes to the total specialization in the resource uptake with an amount in the range $(0, 1)$. The maximum specialization M_{uptake} occurs whenever each of the M_{uptake} relationships results in the specialization in either resource for all individuals. Of course, due to conflicting relations between those variables, this maximum level may never be attained.

From the same plot, it is possible to say that, excluding the range of strongly convex curvatures, a larger resource replenishment rate, ΔR, will usually lead to lower levels of specialization. The scarcity of resources creates more pressure for the population to specialize in the use of different sets of resources (Østman, Lin, and Adami 2014). A similar qualitative dependence is observed for the levels of specialization in high yield. Since, one has N_r pairwise relationships of the class $A_k \times \eta_k$, the maximum possible value of specialization in high yield is N_r. This measurement only accounts for the condition $\eta_k/(A_k/A_{max}) > r_{spec}$, implying it is directional, in the sense only those individuals that specialize in finding a high efficiency in a given resource or given set of resources contribute to the measurement. As we will see, the scenarios displayed by settling $\alpha_{yield} = 0$ are not a rule of great generality. Let us now address the reversed situation, whereby $\alpha_{uptake} = 0$ and varying α_{yield}. The form of how of specialization levels vary with α_{yield} is clearly dependent on the resource input ΔR. While for small ΔR the increase of α_{yield} drive the population to lower levels of specialization, the converse is obtained at large ΔR, with individuals becoming more specialization as α_{yield} rises. Looking at the right

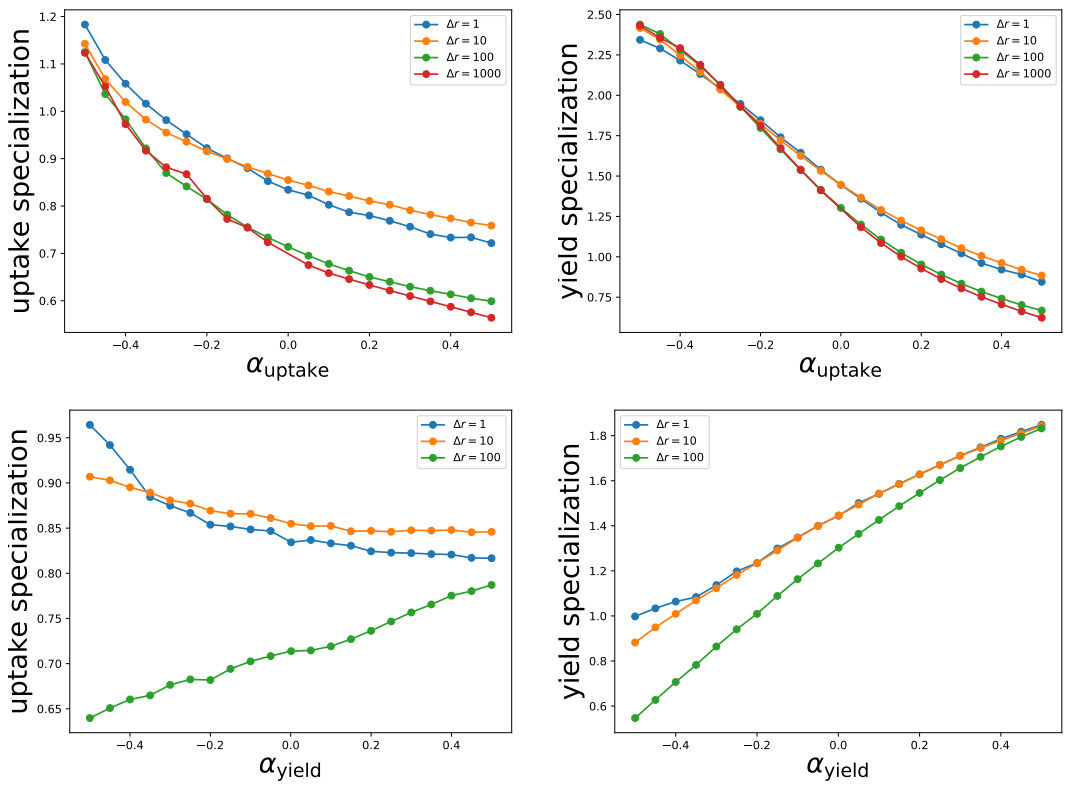

Figure 4: Specialization level for several values of resource input rate ΔR. The left panels depict the specialization level in uptake and the right panels the specialization in yield. In the top panels α_{uptake} varies while α_{yield} is fixed at zero and in the bottom panels α_{yield} varies while α_{uptake} is fixed at zero. dependence with α_{uptake} for constant $\alpha_{\text{yield}} = 0$ and the right panel shows the dependence with α_{yield} for constant $\alpha_{\text{uptake}} = 0$. The parameters are $N = 3$, $\nu = 0.01$, $A_{\max} = 10$, $L = 100$, $D = 0.2$, $\Delta t = 0.1$ and $\Delta x = 1$. Each point consists of an average over 100000 time units, sampled every 5 time units, taken from 50 independent configurations.

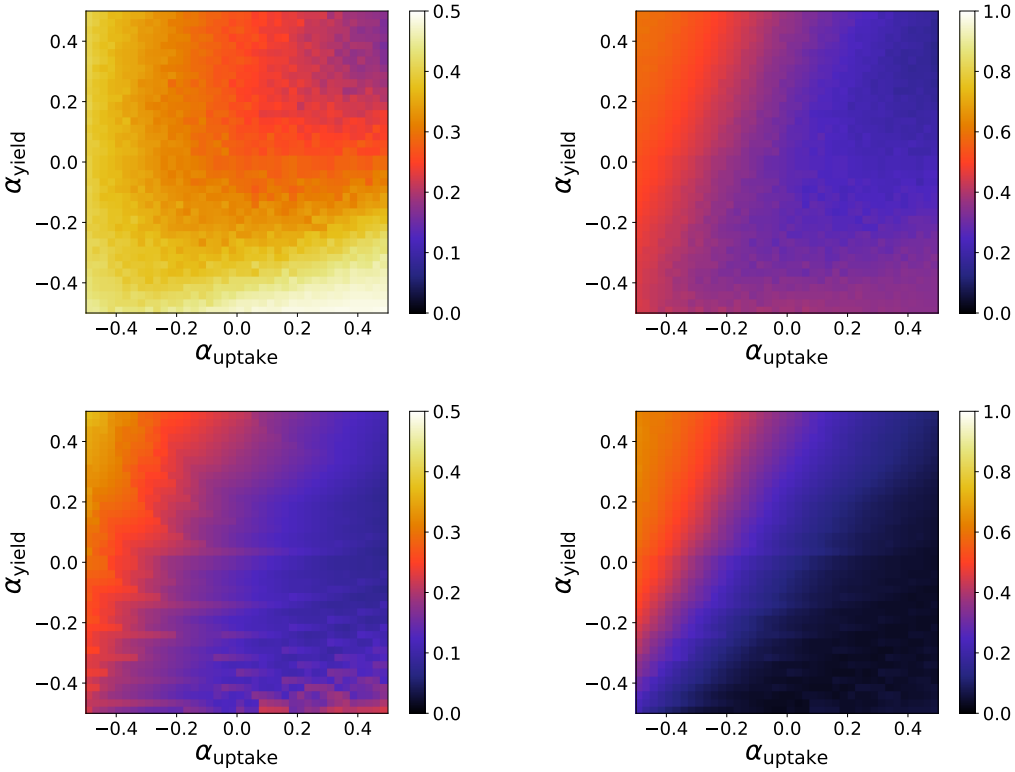

Figure 5: Specialization level for resource input rate $\Delta R = 1$ (top panels) and $\Delta R = 1000$ (bottom panels). The left panels depict the specialization level in uptake and the right panels the specialization in yield. The parameters are $N_r = 2$, $\nu = 0.01$, $A_{\max} = 10$, $L = 100$, $D = 0.2$, $\Delta t = 0.1$ and $\Delta x = 1$. Each point consists of an average over 100000 time units, sampled every 5 time units, taken from 5 independent configurations.

panel of 3, it is possible to relate the growth of specialization with the growth of the population. Meanwhile, the influence of α_{yield} on the specialization in high yield looks much simpler, though quite remarkable. The specialization level advance with α_{yield}, which is somewhat counterintuitive, as positive values of α_{yield} imply that the relations $A_k \times \eta_k$ are described by concave curves, that if lonely considered, would endorse the generalist behavior.

For the sake of simplicity, from now on our assessments for the levels of specialization will be normalized by their maximum possible value, in order to help us for a better judgment about the role of the evolutionary mechanisms under scenarios of a distinct number of resources. Figure 5 presents heat maps for the specialization levels

in both resource uptake and high yield for the number of resources $N_r = 2$ and over a broad domain of the curvature parameters, α_{uptake} and α_{yield}. The upper panels refer to a resource supply rate $\Delta R = 1$, whereas in the lower panels $\Delta R = 1000$. In the range, $\alpha_{yield} \geq -0.1$, the augment of α_{uptake} at fixed α_{yield} yields lower levels of specialization, in accordance with the outcomes shown in Fig. 4. If only discussed from the perspective of the relationship $A_1 \times A_2$, this behavior sounds intuitive, as concave curvatures tend to promote the generalist behavior. Nevertheless, when $\alpha_{uptake} < -0.1$, the scenario is completely modified, with the enlargement of α_{uptake} now boosting specialization in the resource uptake. Thus, there is a loss of generality of the outcomes posed in Figure 4. In this aspect, the issue looks simpler when we probe how the level of specialization in high yield changes with α_{uptake} (right panel). In all the domain, the rise of α_{uptake} dwindles the levels of specialization in high yield.

Let us now scrutinize the response of the specialization to changes of the curvature parameter α_{yield}. As all variables are somehow coupled through the definition of a surface in the $\vec{A}$-subspace, and in its turn the set $\{A_K\}$ are linked to the efficiencies $\{\eta_k\}$ through the N_r relations of the type $A_k \times \eta_k$, α_{yield} is expected to affect the dynamics as a whole. By making α_{uptake} constant, we observe that the rise of the curvature parameter α_{yield}, which turns the tradeoff curves more concave, ensures reduced levels of specialization in the resource uptake (please, see left upper panel of Fig. 5)). On the other hand, a more intricate picture emerges when analyzing the effect of α_{yield} on the specialization in high yield (right panel of Fig. 5). To begin with, looking at the domain of negative values of α_{uptake}, the increment of α_{yield} in almost this domain, counterintuitively, results in enhanced levels of specialization. This is the same pattern seen in Figure 4, which corroborates our previous finding. Differently, in the domain of positive values of α_{uptake}, we can shortly say that the specialization levels in high yield drop off with the augment of α_{yield}, which would be the expected behavior in the absence of other constraints. Note that this regime was not observed in Fig. 4, where the number of resources was set at $N_r = 3$, instead of $N_r = 2$ as in Fig. 5. This way, it is important to see whether the existence of distinct regimes over α_{uptake} is a general rule, or an exception only observed when $N_r = 2$.

The lower panels of Fig. 5 presents the same statistics but now the resource influx rate is $\Delta R = 1000$. In this scenario, the space limitation plays a more prominent role, as the fraction of occupied sites of the lattice is already close to unity. The plots for the specialization levels unveil a less complex structure than before. In fact, the pattern

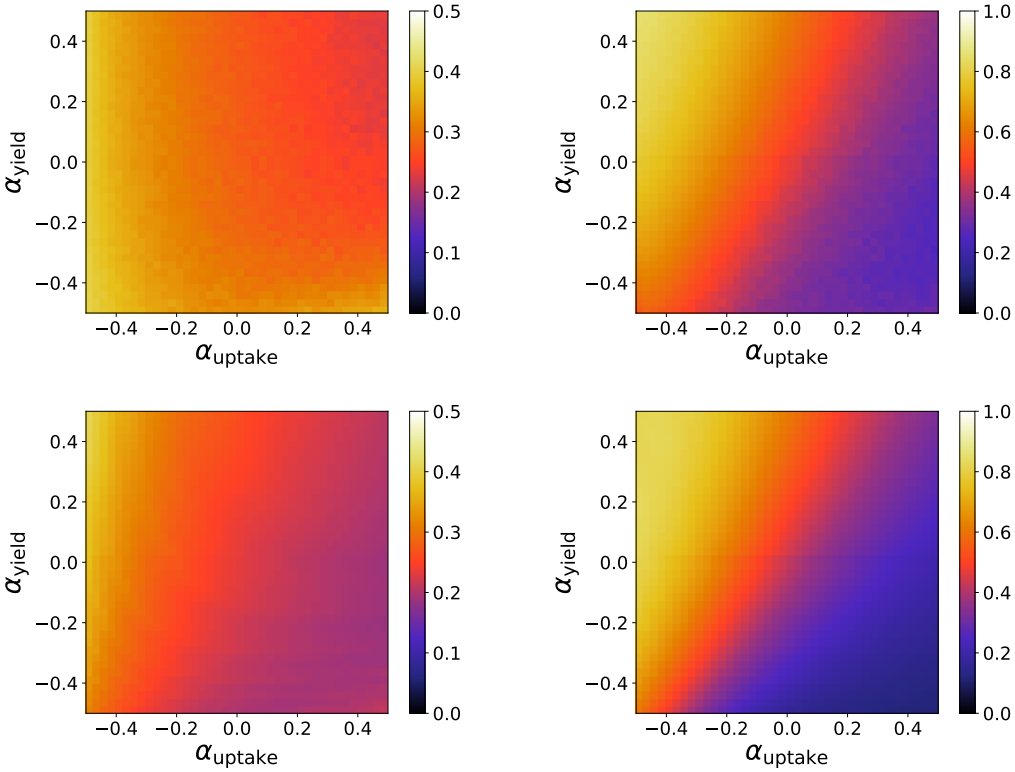

Figure 6: Specialization level for resource input rate $\Delta R = 1$ (top panels) and $\Delta R = 1000$ (bottom panels). The left panels depict the specialization level in uptake and the right panels the specialization in yield. The parameters are $N_r = 3$, $\nu = 0.01$, $A_{\max} = 10$, $L = 100$, $D = 0.2$, $\Delta t = 0.1$ and $\Delta x = 1$. Each point consists of an average over 100000 time units, sampled every 5 time units, taken from 5 independent configurations.

of variation seen in both plots looks very similar. At fixed α_{yield}, the increase of α_{uptake} lowers the specialization in the resource uptake, whereas by holding α_{uptake}, the increment of α_{yield} favors more specialization. The highest levels of specialization in both resource uptake and high yield are achieved in the quadrant defined by $\alpha_{uptake} < 0$ and $\alpha_{yield} > 0$.

In Fig. 6, the same inquiry is carried out but now $N_r = 3$. The resuls are qualitatively very similar to those for $N_r = 2$, but it is important to stress that the peculiar regime seen in the range $\alpha_{yield} \lesssim 0.1$ for $N_r = 2$ and $\Delta R = 1$, is now enclosed in an even narrower domain, $-0.5 \lesssim \alpha_{yield} \lesssim -0.4$. For $N_r = 5$ resources (Fig. 7), this peculiar regime is completely wiped out. An important point to

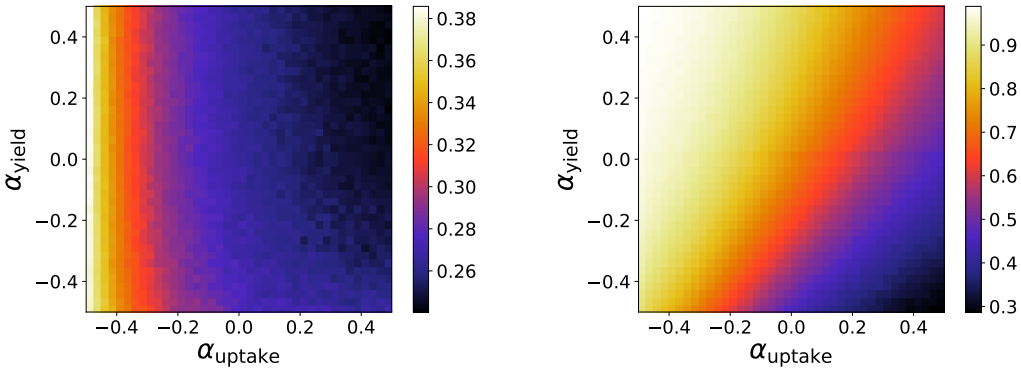

Figure 7: Specialization level for resource input rate $\Delta R = 1$. The left panel depicts the specialization level in uptake and the right panel the specialization in yield. The parameters are $N_r = 5$, $\nu = 0.01$, $A_{\max} = 10$, $L = 100$, $D = 0.2$, $\Delta t = 0.1$ and $\Delta x = 1$. Each point consists of an average over 100000 time units, sampled every 5 time units, taken from 5 independent configurations.

highlight is that for $N_r = 5$ resources, the curvature parameter α_{yield} is much less influential in ruling the levels of specialization in the uptake of resources.

Conclusions

Tradeoff relationships are a critical factor in controlling the degree of functional specialization in natural populations (Michod et al. 2006). From a microevolutionary perspective, this issue has been largely debated within the context of germ-soma differentiation (Michod et al. 2006; Leslie et al. 2017), and also discussed within the context of the evolution of multicellularity (Gavrilets 2010; Ispolatov et al. 2012; Amado and Campos 2017; Amado et al. 2018). A central feature about the tradeoffs is their structure (Jessup and Bohannan 2008; Saeki et al. 2014). Within an ecological viewpoint, the role of the shape of tradeoffs have been related to the emergence of specialists and/or generalists individuals (Egas et al. 2004; Guillaume and Otto 2012), to the levels of biodiversity within communities (Farahpour et al. 2018), and even to their responses to ecological competition (Maharjan et al. 2013). The most diverse forms of tradeoff have been reported, particularly some of those describing relationships between life-history traits are well established in the literature (Jessup and Bohannan 2008; Saeki et al. 2014).

Nevertheless, the usual approach to describe the tradeoff as single

curves relating any two traits that are implicitly subject to biological and biophysical constraints are no longer suitable in case those traits are mediated by other mechanisms or traits. Therefore, a proper description of such cases requires a multivariate analysis to properly address the complex structure of trait spaces (Edwards and Stachowicz 2010; Edwards et al. 2011). Here, we have assumed the existence of multivariate tradeoff patterns to address the development of functional specialization. The traits comprising the trait space are associated with the metabolic properties of the individuals, more specifically, their resource uptake rates and corresponding efficiencies. The current resolution allows us to observe how the structure of the multidimensional tradeoffs regulates the levels of specialization in a scenario where those traits are intertwined and compare how the new predictions compare to classical ecological studies of two traits. The levels of functional specialization are studied in a scenario of a harsh environment, e.g. low resource influx rate, as well as in a scenario whereby resources abound. Moreover, a thorough survey of how the shape of the tradeoff relationships affect specialization is accomplished.

The first important observation is that population sizes are very little influenced by the efficiency of the metabolic machinery, but rather are strongly determined by the curvature of the subspace of resource uptake rates $\vec{A} = (A_1, A_2, \ldots, A_{N_r})$. In our formulation, the concavity of the surface relating the set of values $\{A_k\}$ is handled by the parameter α_{uptake}. Negative values of α_{uptake} generates convex surfaces in that subspace, whereas positive values of α_{uptake} create concave surfaces. Our knowledge from classical ecological models suggests that in two-trait models that specialization is facilitated upon convex tradeoff curves (Egas et al. 2004; Hoyle et al. 2008). The simulation results show that population size increases as the tradeoff surface becomes more convex, i.e., when α_{uptake} is lowered. In fact, the highest levels of functional specialization in the uptake of resources is found in the realm of negative values of α_{uptake}. An exception to this rule is the case $N_r = 2$, in which considerable large levels of specialization are also achieved for positive α_{uptake} when the second curvature parameter α_{yield}, ruling the relation $A_k \times \eta_k$, is very negative (de Oliveira et al. 2018). This peculiar regime, verified for $N_r = 2$, clearly contradicts our common sense gleaned from the classical models of two-traits. Even peculiar, this regime is our first evidence that the interplay of tradeoffs can lead to quite unexpected outcomes.

Now, overlooking the tradeoff between uptake rates, we would expect that lower levels of specialization would be achieved under concave tradeoff curves ($\alpha_{yield} > 0$), in either direction, uptake rate or

high efficiency. In fact, we observe the reversed situation, and thereby the highest levels of specialization in high yield occurs in the domain of positive values of α_{yield}. To be more precise, specialization in high yield ensues in the quad $\alpha_{yield} < 0$ together with $\alpha_{uptake} < 0$. This situation is exactly the same irrespective of the number of resources, N_r, as well as the resource input, ΔR.

The fact that the domain in which the greatest levels of specialization in high yield appears coincides with that in which the specialization in the uptake of resources is also favored, seems to suggest that the tradeoff among the set of resource uptake rates $\{A_k\}$, with $k = 1, \ldots, N_r$ is prevailing over the class of tradeoffs $A_k \times \eta_k$, as it is even more noticeable in the range $\alpha_{uptake} < 0$ (convex surface) and ($\alpha_{yield} > 0$) (concave curves). Note that this region of high specialization in high yield is broadened as α_{yield} is further augmented, which also suggests that somehow there is a reduction of conflicting positions among the variables. The realm of high specialization in both resource uptake and high yield portrays the scenario in which the individuals evolve to high rates of resource uptake for a subset of resource types while handling a complementary subset with high efficiency.

The essence that the tradeoffs over the set of resource uptake rates $\{A_k\}$ overrule the dynamics of the system, our results also demonstrate that there is room for a clear manifestation of the class of tradeoffs $A_k \times \eta_k$, which is verified when $\alpha_{yield} < 0$ and $\alpha_{uptake} > 0$, and following the same reasoning hints a situation of less conflicting conditions over all the metabolic variables. However, opposed to the scenario portrayed in the previous paragraph, this peculiar regime is particularly verified under conditions of low resource availability and a small number of resources.

Acknowledgments

PRAC acknowledges financial support from Fundação de Amparo à Ciência e Tecnologia do Estado de Pernambuco (FACEPE) under Project No. APQ-0464-1.05/15, and Conselho Nacional de Desenvolvimento Científico e Tecnológico (CNPq) under Projects No. 303497/2014-9 and 406594/2018-0. AA has a fellowship from the program PNPD sponsored by Coordenação de Aperfeiçoamento de Pessoal de Nível Superior (CAPES).

References

Amado, A., C. Batista, and P. R. Campos (2018). A theoretical approach to the size-complexity rule. *Evolution 72*(1), 18–29.

Amado, A. and P. R. Campos (2017). The influence of the composition of tradeoffs on the generation of differentiated cells. *Journal of Statistical Mechanics: Theory and Experiment 2017*(6), 063501.

Beier, S., A. R. Rivers, M. A. Moran, and I. Obernosterer (2015). Phenotypic plasticity in heterotrophic marine microbial communities in continuous cultures. *The ISME journal 9*(5), 1141.

Campbell, M. and S. Farrell (2006). Biochemistry; 2 th. *Boston, Mass, USA: Cengage Learning*.

Chen, Q. and G. Wang (2003). A class of bézier-like curves. *Computer Aided Geometric Design 20*(1), 29–39.

Chevin, L.-M., R. Gallet, R. Gomulkiewicz, R. D. Holt, and S. Fellous (2013). Phenotypic plasticity in evolutionary rescue experiments. *Philosophical Transactions of the Royal Society of London B: Biological Sciences 368*(1610), 20120089.

de Oliveira, V. M., A. Amado, and P. R. Campos (2018). The interplay of tradeoffs within the framework of a resource-based modelling. *Ecological Modelling 384*, 249–260.

Edwards, K. F., C. A. Klausmeier, and E. Litchman (2011). Evidence for a three-way trade-off between nitrogen and phosphorus competitive abilities and cell size in phytoplankton. *Ecology 92*(11), 2085–2095.

Edwards, K. F. and J. J. Stachowicz (2010). Multivariate trade-offs, succession, and phenological differentiation in a guild of colonial invertebrates. *Ecology 91*(11), 3146–3152.

Egas, M., U. Dieckmann, and M. W. Sabelis (2004). Evolution restricts the coexistence of specialists and generalists: the role of trade-off structure. *The American Naturalist 163*(4), 518–531.

Farahpour, F., M. Saeedghalati, V. S. Brauer, and D. Hoffmann (2018). Trade-off shapes diversity in eco-evolutionary dynamics. *eLife 7*, e36273.

Farin, G., J. Hoschek, and M.-S. Kim (2002). *Handbook of computer aided geometric design*. Elsevier.

Ferenci, T. (2016). Trade-off mechanisms shaping the diversity of bacteria. *Trends in microbiology 24*(3), 209–223.

Garland, T. (2014). Trade-offs. *Current Biology 24*(2), R60–R61.

Gavrilets, S. (2010). Rapid transition towards the division of labor via evolution of developmental plasticity. *PLoS Comput*

Biol 6(6), e1000805.

Ghalambor, C. K., J. K. McKay, S. P. Carroll, and D. N. Reznick (2007). Adaptive versus non-adaptive phenotypic plasticity and the potential for contemporary adaptation in new environments. *Functional ecology 21*(3), 394–407.

Ghoul, M. and S. Mitri (2016). The ecology and evolution of microbial competition. *Trends in microbiology 24*(10), 833–845.

Gibbons, S. M. and J. A. Gilbert (2015). Microbial diversityexploration of natural ecosystems and microbiomes. *Current opinion in genetics & development 35*, 66–72.

Guillaume, F. and S. P. Otto (2012). Gene functional trade-offs and the evolution of pleiotropy. *Genetics*, genetics–112.

Hibbing, M. E., C. Fuqua, M. R. Parsek, and S. B. Peterson (2010). Bacterial competition: surviving and thriving in the microbial jungle. *Nature Reviews Microbiology 8*(1), 15.

Hoyle, A., R. G. Bowers, A. White, and M. Boots (2008). The influence of trade-off shape on evolutionary behaviour in classical ecological scenarios. *Journal of Theoretical Biology 250*(3), 498–511.

Ispolatov, I., M. Ackermann, and M. Doebeli (2012). Division of labour and the evolution of multicellularity. *Proceedings of the Royal Society of London B: Biological Sciences 279*(1734), 1768–1776.

Jessup, C. M. and B. J. Bohannan (2008). The shape of an ecological trade-off varies with environment. *Ecology Letters 11*(9), 947–959.

Kelly, S. A., T. M. Panhuis, and A. M. Stoehr (2012). Phenotypic plasticity: molecular mechanisms and adaptive significance. *Compr Physiol 2*(2), 1417–39.

Kneitel, J. M. and J. M. Chase (2004). Trade-offs in community ecology: linking spatial scales and species coexistence. *Ecology Letters 7*(1), 69–80.

Kümmerli, R., N. Jiricny, L. Clarke, S. West, and A. Griffin (2009). Phenotypic plasticity of a cooperative behaviour in bacteria. *Journal of evolutionary biology 22*(3), 589–598.

Lancaster, L., L. Hazard, J. Clobert, and B. Sinervo (2008). Corticosterone manipulation reveals differences in hierarchical organization of multidimensional reproductive trade-offs in r-strategist and k-strategist females. *Journal of evolutionary biology 21*(2), 556–565.

Leslie, M. P., D. E. Shelton, and R. E. Michod (2017). Generation

time and fitness tradeoffs during the evolution of multicellularity. *Journal of theoretical biology 430*, 92–102.

Litchman, E., K. F. Edwards, and C. A. Klausmeier (2015). Microbial resource utilization traits and trade-offs: implications for community structure, functioning, and biogeochemical impacts at present and in the future. *Frontiers in microbiology 6*.

Maharjan, R., S. Nilsson, J. Sung, K. Haynes, R. E. Beardmore, L. D. Hurst, T. Ferenci, and I. Gudelj (2013). The form of a trade-off determines the response to competition. *Ecology letters 16*(10), 1267–1276.

Matesanz, S., E. Gianoli, and F. Valladares (2010). Global change and the evolution of phenotypic plasticity in plants. *Annals of the New York Academy of Sciences 1206*(1), 35–55.

Michod, R. E., Y. Viossat, C. A. Solari, M. Hurand, and A. M. Nedelcu (2006). Life-history evolution and the origin of multicellularity. *Journal of theoretical Biology 239*(2), 257–272.

Nicotra, A. B., O. K. Atkin, S. P. Bonser, A. M. Davidson, E. Finnegan, U. Mathesius, P. Poot, M. D. Purugganan, C. L. Richards, F. Valladares, et al. (2010). Plant phenotypic plasticity in a changing climate. *Trends in plant science 15*(12), 684–692.

Østman, B., R. Lin, and C. Adami (2014). Trade-offs drive resource specialization and the gradual establishment of ecotypes. *BMC evolutionary biology 14*(1), 113.

Pease, C. and J. Bull (1988). A critique of methods for measuring life history trade-offs. *Journal of Evolutionary Biology 1*(4), 293–303.

Pfeiffer, T., S. Schuster, and S. Bonhoeffer (2001). Cooperation and competition in the evolution of atp-producing pathways. *Science 292*(5516), 504–507.

Rockwood, L. L. (2015). *Introduction to population ecology*. John Wiley & Sons.

Saeki, Y., M. Tuda, and P. H. Crowley (2014). Allocation tradeoffs and life histories: a conceptual and graphical framework. *Oikos 123*(7), 786–793.

Sultan, S. E. and H. G. Spencer (2002). Metapopulation structure favors plasticity over local adaptation. *The American Naturalist 160*(2), 271–283.

Valladares, F., S. Matesanz, F. Guilhaumon, M. B. Araújo, L. Balaguer, M. Benito-Garzón, W. Cornwell, E. Gianoli, M. van Kleunen, D. E. Naya, et al. (2014). The effects of phenotypic plas-

ticity and local adaptation on forecasts of species range shifts under climate change. *Ecology letters 17*(11), 1351–1364.